Article

Neuron

A Temporary Gating of Actin Remodeling during Synaptic Plasticity Consists of the Interplay between the Kinase and Structural Functions of CaMKII

Highlights

- CaMKII stabilizes F-actin by limiting access of actin modulators within the spine
- CaMKII detaches from F-actin by autophosphorylation right after LTP induction
- Actin regulators modify actin cytoskeleton upon CaMKII detachment
- CaMKII quickly reassociates and stabilizes F-actin during LTP maintenance

Authors

Karam Kim, Gurpreet Lakhanpal, Hsiangmin E. Lu, ..., Thomas A. Blanpied, Yasunori Hayashi, Kenichi Okamoto

Correspondence

yhayashi@brain.riken.jp (Y.H.), okamoto@lunenfeld.ca (K.O.)

In Brief

Kim et al. demonstrate autophosphorylation-mediated F-actin regulation of CaMKII during synaptic plasticity of a dendritic spine. Its enzymatic and structural functions are linked to regulate the modification of actin cytoskeleton to prevent unnecessary change in spine structure and synaptic transmission.

Kim et al., 2015, Neuron *87*, 813–826
August 19, 2015
http://dx.doi.org/10.1016/j.neuron.2015.07.023

CellPress

Neuron
Article

A Temporary Gating of Actin Remodeling during Synaptic Plasticity Consists of the Interplay between the Kinase and Structural Functions of CaMKII

Karam Kim,[1] Gurpreet Lakhanpal,[2] Hsiangmin E. Lu,[3,4] Mustafa Khan,[2] Akio Suzuki,[1] Mariko Kato Hayashi,[6] Radhakrishnan Narayanan,[6] Thomas T. Luyben,[2,7] Tomoki Matsuda,[8] Takeharu Nagai,[8] Thomas A. Blanpied,[3,4,5] Yasunori Hayashi,[1,6,9,10,11,*] and Kenichi Okamoto[2,6,7,11,*]
[1]Brain Science Institute, RIKEN, Wako, Saitama 351-0198, Japan
[2]Lunenfeld-Tanenbaum Research Institute, Mount Sinai Hospital, Toronto, ON, M5G 1X5, Canada
[3]Department of Physiology
[4]Program in Molecular Medicine
[5]Program in Neuroscience
University of Maryland School of Medicine, Baltimore, MD 21201, USA
[6]RIKEN-MIT Neuroscience Research Center, The Picower Institute for Learning and Memory, Department of Brain and Cognitive Sciences, Massachusetts Institute of Technology, Cambridge, MA 02139, USA
[7]Department of Molecular Genetics, Faculty of Medicine, University of Toronto, Toronto, ON, M5S 1A8, Canada
[8]The Institute of Scientific and Industrial Research, Osaka University, Osaka 567-0047, Japan
[9]Brain and Body System Science Institute, Saitama University, Saitama 338-8570, Japan
[10]School of Life Science, South China Normal University, Guangzhou 510631, China
[11]Co-senior author
*Correspondence: yhayashi@brain.riken.jp (Y.H.), okamoto@lunenfeld.ca (K.O.)
http://dx.doi.org/10.1016/j.neuron.2015.07.023

SUMMARY

The structural modification of dendritic spines plays a critical role in synaptic plasticity. CaMKII is a pivotal molecule involved in this process through both kinase-dependent and independent structural functions, but the respective contributions of these two functions to the synaptic plasticity remain unclear. We demonstrate that the transient interplay between the kinase and structural functions of CaMKII during the induction of synaptic plasticity temporally gates the activity-dependent modification of the actin cytoskeleton. Inactive CaMKII binds F-actin, thereby limiting access of actin-regulating proteins to F-actin and stabilizing spine structure. CaMKII-activating stimuli trigger dissociation of CaMKII from F-actin through specific autophosphorylation reactions within the F-actin binding region and permits F-actin remodeling by regulatory proteins followed by reassociation and restabilization. Blocking the autophosphorylation impairs both functional and structural plasticity without affecting kinase activity. These results underpin the importance of the interplay between the kinase and structural functions of CaMKII in defining a time window permissive for synaptic plasticity.

INTRODUCTION

The spine is a tiny protrusive structure on a dendrite that harbors an excitatory synapse. Induction of synaptic plasticity leads to long-term structural changes of the spine. LTP-inducing stimuli lead to an increase in spine size (structural LTP or sLTP), while LTD-inducing stimuli cause spines to shrink (reviewed in Bosch and Hayashi, 2012). There is a tight relationship between the size of a spine and strength of synaptic transmission (Harris et al., 1992; Schikorski and Stevens, 1997; Matsuzaki et al., 2001), and, therefore, the structural plasticity of a spine is considered a crucial process of synaptic plasticity.

The actin cytoskeleton plays a pivotal role in regulating spine shape (Pontrello and Ethell, 2009; Hotulainen and Hoogenraad, 2010). Actin undergoes constant treadmilling from the periphery toward the center of the spine head, maintaining the structure of each spine (Honkura et al., 2008; Frost et al., 2010). During LTP induction, the balance between filamentous (F-) actin formation and degradation is transiently shifted. NMDA-R-driven activation of cofilin severs existing F-actin within the spine, and the Arp2/3 complex is recruited (Hotulainen and Hoogenraad, 2010; Bosch et al., 2014; Calabrese et al., 2014). Both mechanisms generate new sites from which additional filaments can grow, resulting in an elevation of F-actin content and spine enlargement. Interestingly, stimuli that leave no lasting influence on synaptic transmission can induce a transient and reversible increase in spine F-actin content (Okamoto et al., 2004). However, LTP is characterized by a shift to new, elevated steady-state levels of F-actin content, which persistently supports the enlarged spine structure (Okamoto et al., 2004; Bosch et al., 2014). Therefore, during LTP induction, F-actin undergoes a biphasic reaction characterized by an initial reorganization, followed by a restabilization phase.

The critical trigger for LTP is the influx of Ca^{2+} through the NMDA-R and the resultant activation of Ca^{2+}/calmodulin-dependent protein kinase II (CaMKII). Both of these components work within a defined time window during LTP induction. Ca^{2+} is

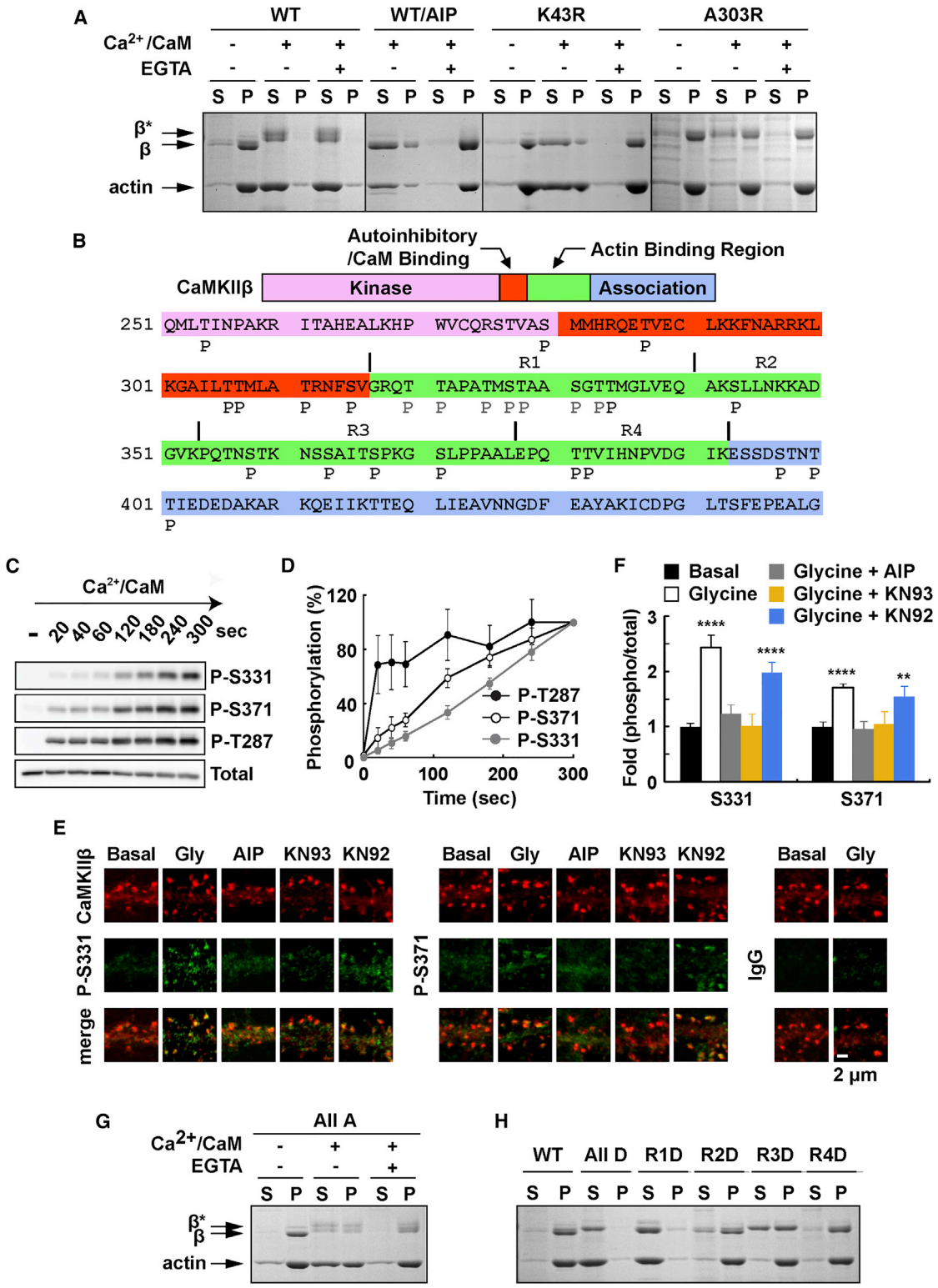

Figure 1. Autophosphorylation of the F-Actin Binding Region Dissociates CaMKIIβ from F-Actin

(A) CaMKIIβ activation and subsequent autophosphorylation negatively regulates the interaction of CaMKIIβ with F-actin. Purified CaMKIIβ from Sf9 or HEK293T cells were incubated with purified F-actin from human platelets for 5 min with or without 50 μM autocamtide-2-related inhibitory peptide (AIP). CaMKIIβ was activated by Ca^{2+}, calmodulin, and ATP (Ca^{2+}/CaM), followed by incubation for another 5 min. The reaction was then continued with or without EGTA for 20 min.

(legend continued on next page)

required only during the first second after LTP induction (Malenka et al., 1992). CaMKII activity lasts for ~1 min after LTP induction and soon returns to the basal level, unlike previously hypothesized (Chen et al., 2001; Lee et al., 2009; Lisman et al., 2012). The unique temporal actions of these and other molecular processes likely relate to the distinct properties of synapses at different phases following LTP induction. A potentiated synapse is labile during the first few minutes after LTP induction and is easily depotentiated upon low frequency stimulation. Thereafter, the synapse gradually becomes resistant to input modulation and is eventually consolidated (Huang and Hsu, 2001). The mechanisms whereby transient cellular signals are converted into a persistent enhancement of synaptic function and how such signals shape different phases of synaptic plasticity still remain elusive.

CaMKII is situated upstream of the signaling leading to F-actin modification and contributes to synaptic plasticity through kinase-dependent and independent, structural functions. It phosphorylates various postsynaptic proteins including guanine nucleotide exchange factors (GEFs), which leads to actin modification (Saneyoshi and Hayashi, 2012). Also, CaMKII phosphorylates and activates LIM kinase, a major regulator of actin (Saito et al., 2013). In addition to these signaling roles, accumulating evidence suggests that CaMKII holoenzyme itself also functions as a structural element at the synapse (Okamoto et al., 2007, 2009; Hell, 2014). For instance, downregulation of CaMKIIβ converts spines into filopodia (Okamoto et al., 2007), an effect that can be fully rescued by a kinase null mutant of CaMKIIβ, and thus is independent of kinase activity. Such action is believed to be possible because CaMKIIβ binds and crosslinks F-actin through its dodecameric structure (O'Leary et al., 2006; Okamoto et al., 2007; Lin and Redmond, 2008; Sanabria et al., 2009). Interestingly, active CaMKIIβ detaches from F-actin, allowing its unbundling (Fink et al., 2003; O'Leary et al., 2006; Okamoto et al., 2007). This is counterintuitive, because CaMKII translocates to the synapse after LTP induction (Shen and Meyer, 1999; Bosch et al., 2014) and F-actin stabilization depends on CaMKII activity (Okamoto et al., 2004; Honkura et al., 2008). While dynamic rearrangement of CaMKII in the postsynaptic compartment has been reported, it remains unclear how kinase-dependent and independent functions are temporally regulated and how each contributes to specific aspects of F-actin rearrangement and stabilization.

In this study, we discovered an autophosphorylation-mediated mechanism of CaMKII that regulates its structural function. We identified and characterized the autophosphorylation sites on CaMKII that regulate F-actin stability during brief periods of activation, not just by CaMKII-actin linkage but by controlling the access of actin regulatory molecules to F-actin. The autophosphorylation of CaMKII detaches it from F-actin and thereby opens a brief time window for actin remodeling. Reassociation of CaMKII with F-actin closes the time window and stabilizes the new F-actin structure for extended periods of time. In light of these findings, we propose that CaMKII serves as a general inhibitor of F-actin remodeling in spines, whose activity is negatively regulated by Ca^{2+}/calmodulin (CaM) binding and by the resultant autophosphorylation within a limited time period after LTP induction. This function of CaMKII links transient cellular signaling to persistent, long-term changes in synaptic strength by establishing a molecular-temporal gate for synaptic plasticity.

RESULTS

Phosphorylation Sites on the F-Actin Binding Region of CaMKIIβ Regulate CaMKII-F-Actin Interaction

We first examined the interplay between the kinase activity and the F-actin binding ability of CaMKIIβ using an in vitro reconstituted system. CaMKIIβ was first allowed to interact with F-actin and then stimulated with Ca^{2+}/CaM. After 5 min, Ca^{2+} was chelated by EGTA, and the mixture was further incubated. Finally, the bundled and unbundled F-actin were separated by centrifugation and subjected to SDS-PAGE. Consistent with previous results, when CaMKIIβ was activated by Ca^{2+}, a decrease in the binding to F-actin was observed (Figure 1A) (Fink et al., 2003; O'Leary et al., 2006; Okamoto et al., 2007). The decreased levels of binding persisted after the chelation of Ca^{2+} with EGTA. To test the respective contribution of Ca^{2+}/CaM-binding per se and resultant kinase activation to the detachment, we used a kinase inhibitor or CaMKIIβ mutants deficient in kinase activity or CaM binding. Autocamtide-2-related inhibitory peptide (AIP), a peptide inhibitor of CaMKII, did not change the detachment caused by Ca^{2+} but blocked the persistent detachment after

The mixtures were centrifuged at low speed so that only bundled F-actin precipitates while unbundled F-actin remains in the supernatant. The supernatant (S) and pellet (P) fractions were subjected to SDS-PAGE and stained with Coomassie brilliant blue. WT, wild-type; K43R, kinase null mutant; A303R, CaM-binding-deficient mutant. β* indicates band-shifted population because of phosphorylation. A303R is larger than others because of the purification tag.

(B) Results of LC-MS/MS analysis of CaMKIIβ phosphorylation. R1-R4 is based on splice variants. See Figures S1A and S1B and Table S1 for full details.

(C) Time course of phosphorylation at T287, S331, and S371.

(D) Quantification of band intensities in (C), n = 3.

(E) Phosphorylation of S331 and S371 of endogenous CaMKIIβ. Dissociated hippocampal neurons were treated with 200 μM glycine for 3 min and stained with phospho-specific and CaMKIIβ antibodies. Before stimulation, neurons were preincubated for 1 hr with 10 μM of each inhibitor.

(F) Quantification of fluorescence intensity of spines in (E). The intensity of the phospho-specific antibody channel was normalized to that of the CaMKIIβ antibody channel in each spine to cancel out the accumulation of CaMKIIβ after stimulation. n = 18/17 (basal), 15/20 (glycine), 12/9 (AIP), 6/8 (KN-93), and 13/16 (KN-92) neurons for P-S331/P-S371. Ten to twenty spines were quantified from each neuron. Kruskal-Wallis test followed by Mann-Whitney U test with Bonferroni correction was used.

(G) Phosphoblock All A mutant in the F-actin binding region partly detached from F-actin in the presence of Ca^{2+}/CaM but reassociated with F-actin upon chelation of Ca^{2+}. The upward band-shift by Ca^{2+} stimulation confirms that All A was autophosphorylated at the remaining residues.

(H) Phosphomimetic mutations on the F-actin binding region (All D) abolished F-actin binding activity. Experiments using narrower region-specific phosphomimetic mutants (R1D-R4D, see B) showed that a region between amino acids 317–340 was mainly responsible for regulation of F-actin binding. Purified CaMKIIβ mutants proteins from Sf9 were used in (G) and (H). See also Figure S1.

All error bars represent SEM.

the chelation of Ca^{2+}. Similarly, a kinase null K43R mutant partially detached from F-actin in the presence of Ca^{2+} but fully reassociated after addition of EGTA. A CaM binding-deficient mutant, A303R, retained the ability to bind F-actin with or without Ca^{2+}. Together, the F-actin binding ability of CaMKIIβ is negatively regulated by two mechanisms: one by binding to Ca^{2+}/CaM and another by a kinase-mediated mechanism. The effect of Ca^{2+}/CaM is reversible and possibly arises from steric hindrance between Ca^{2+}/CaM and F-actin binding, as two domains for these interactions are adjacent to each other (Figure 1B). In contrast, the effect of the kinase-mediated mechanism persists even after Ca^{2+} subsides.

CaMKII can be autophosphorylated at multiple sites. Therefore, autophosphorylation is a plausible mechanism for kinase-activity regulated F-actin binding in a system reconstituted from purified proteins. However, with the exception of threonine (T) 286 and T305/T306 (the numbering in α subunit), the role of these autophosphorylation sites is unclear. We therefore carried out mass-spectrometric phosphopeptide mapping. Purified CaMKIIβ was activated with Ca^{2+}/CaM. EGTA was then added to further induce Ca^{2+}/CaM-independent autophosphorylation reaction. At various time points during these steps, the reaction was sampled and subjected to mass spectrometry. This identified multiple sites, many of which are located within the F-actin binding region and conserved among vertebrate species (Figure 1B; see Figures S1A–S1C and Table S1, available online). Some of them were also identified in previous studies using brain-derived protein (Miller et al., 1988; Trinidad et al., 2005; Baucum et al., 2015) (Figure S1B, underlined).

To examine the properties of phosphorylation on the F-actin binding region of CaMKIIβ, we raised phospho-specific antibodies against serine (S) 331 and 371 (Figure S1D). Compared with the phosphorylation of T287, an essential site for constitutive activation (comparable with T286 in CaMKIIα), the phosphorylation of S331 and S371 was slower (Figures 1C and 1D) (Miller et al., 1988). Searching for in vivo evidence of the phosphorylation of these sites, we stimulated dissociated hippocampal neurons with glycine, which has been shown to potentiate synaptic transmission and enlarge spines (Lu et al., 2001; Bosch et al., 2014) and immunostained using the phosphospecific antibodies. The stimulation increased the phosphorylation of both S331 and S371, which was blocked by CaMKII inhibitor AIP and KN-93, but not by an inactive analog, KN-92, confirming that the phosphorylation at these sites is mediated by autophosphorylation, but not other kinases activated by glycine treatment (Figures 1E and 1F). In conclusion, we found multiple autophosphorylation sites within the F-actin binding region of CaMKIIβ. It is thus tempting to speculate on the roles of these sites in the regulation of CaMKII-F-actin interaction.

Autophosphorylation Sites on the F-Actin Binding Region of CaMKIIβ Regulate Interaction with F-Actin

To test if phosphorylation at the F-actin binding region is necessary to regulate the interaction with F-actin, we generated a phosphoblock All A mutant where all S and T residues within the F-actin binding region were changed to alanine, and tested its F-actin binding ability (Figure 1G). The purified All A mutant showed F-actin binding comparable to WT in the absence of Ca^{2+}/CaM. With Ca^{2+}/CaM, All A showed a decrease in F-actin binding. However, whereas the F-actin binding of WT was lost even after Ca^{2+} chelation (Figure 1A), F-actin binding of All A was restored to the levels of the unstimulated kinase (Figure 1G).

In order to further test if the phosphorylation is sufficient to detach CaMKIIβ from F-actin, we made a phosphomimic All D mutant, where the same S and T residues were changed to aspartic acid; we also created narrower regional mutants R1D-R4D, based on splice variants of CaMKIIβ (Figure 1B) (Brocke et al., 1999). The purified All D mutant completely lost F-actin binding activity, similar to the autophosphorylated WT (Figure 1H). Within this region, phosphorylation at R1 is crucial for regulating F-actin binding and to a lesser extent, R3, consistent with a study using splice variants of CaMKIIβ (O'Leary et al., 2006). We confirmed that both All A and All D mutations had no effect on kinase activity toward an exogenous substrate (Figure S1E). These data suggest that phosphorylation at the F-actin binding region is necessary and sufficient to prevent the persistent interaction with F-actin.

CaMKIIβ Inhibits Interactions between F-Actin and Actin-Regulating Proteins

We next tested the impact of F-actin binding of CaMKIIβ on functional regulation of actin. We hypothesized that F-actin-CaMKIIβ interaction limits access of actin-regulating proteins, thereby inhibiting their actions. The dissociation of CaMKIIβ from F-actin by autophosphorylation would permit structural modification by actin-regulating proteins. To test this possibility, we monitored the activity of several actin-regulating proteins with or without CaMKIIβ. In a high-speed sedimentation assay, all the F-actin is collected in the pellet, and any actin remaining in the supernatant is considered as G-actin. Therefore, this assay tests the effect of a given protein on actin polymerization/depolymerization in addition to F-actin binding of the test protein.

We first tested cofilin-1, a ubiquitous actin-depolymerizing protein playing essential roles in many actin-related processes including LTP (Pontrello and Ethell, 2009; Bosch et al., 2014; Calabrese et al., 2014) (Figures 2A and 2B). The treatment of F-actin with cofilin resulted in the recovery of G-actin in the supernatant consistent with the actin severing function of cofilin. Preincubating F-actin with CaMKIIβ reduces the amount of severed actin by 50% (from 55.5% ± 2% to 27.7% ± 0.5%), suggesting that F-actin-cofilin interaction was inhibited by CaMKIIβ (Figures 2A and 2B). In a pyrene-actin assay, we also observed that CaMKIIβ prevented cofilin-induced actin depolymerization (Figure 2C). Of note, CaMKIIβ alone has no effect on actin depolymerization (Figures 2A–2C). This rules out the possibility that CaMKIIβ directly affects the depolymerization and confirms that CaMKIIβ indeed reduces the cofilin-mediated F-actin depolymerization by preventing the interaction between these proteins.

We also tested the interaction of actin with Arp2/3, an actin-nucleating and branching protein complex, and gelsolin, a Ca^{2+}-dependent F-actin severing protein, both implicated in synaptic plasticity and the maintenance of dendritic spine structure (Pontrello and Ethell, 2009; Hotulainen and Hoogenraad, 2010). In a pyrene-actin assay, Arp2/3 complex showed enhanced actin polymerization when combined with an Arp2/3 activator, WASP. However, CaMKIIβ abolished this effect

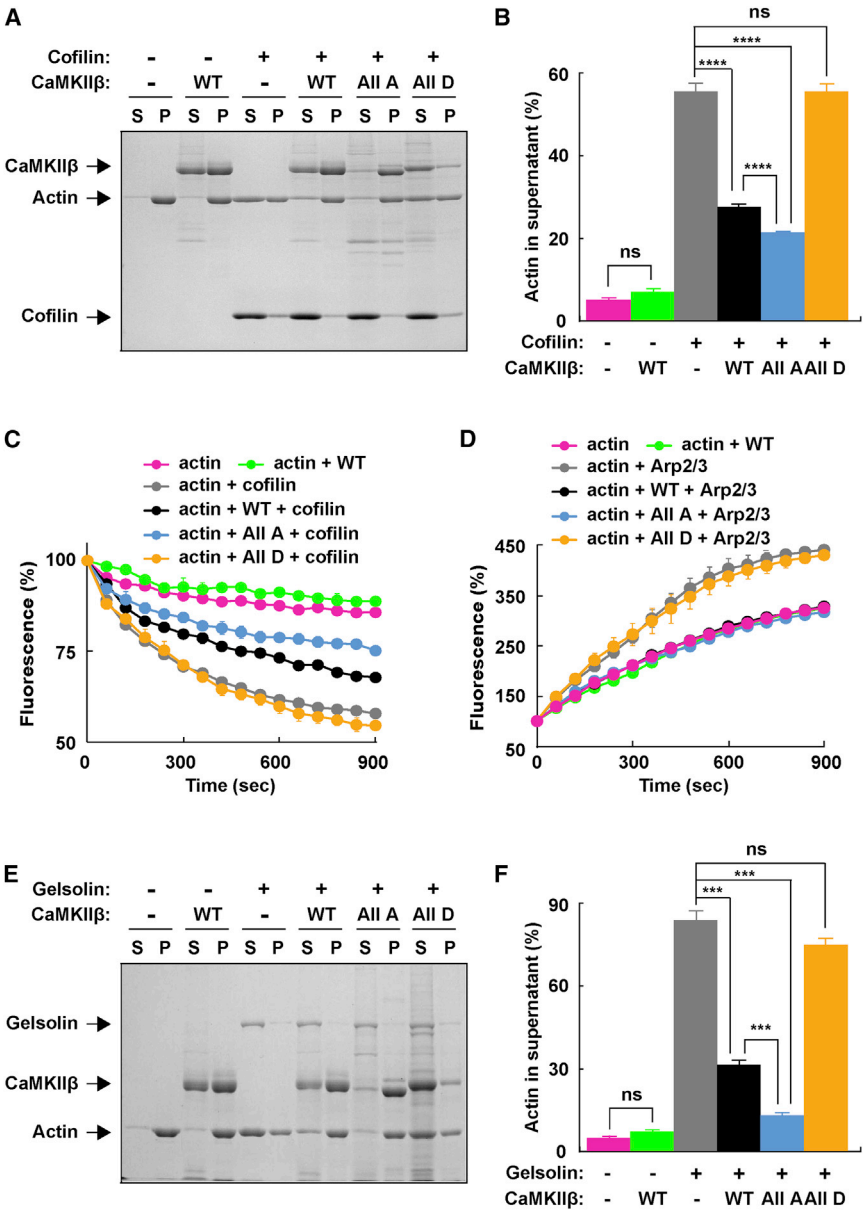

Figure 2. CaMKIIβ Inhibits the Interaction of Actin Binding Proteins with Actin

(A and B) CaMKIIβ inhibits the F-actin severing activity of cofilin. F-actin was incubated with or without CaMKIIβ for 30 min before cofilin was added. After 5 min, the mixture was ultracentrifuged at high speed, and supernatant (S) and pellet (P) fractions were separated on SDS-PAGE. n = 9.

(C) CaMKIIβ slows down F-actin depolymerization by cofilin. F-actin (5% pyrene-labeled) was preincubated with or without CaMKIIβ for 20 min, and dilution-induced depolymerization was monitored in the presence or absence of cofilin, n = 9 (actin, actin+cofilin), 4 (actin+All A+cofilin), 3 (others).

(D) CaMKIIβ inhibits the actin nucleating activity of the Arp2/3 complex. Polymerization of G-actin was recorded with the Arp2/3 complex and VCA domain of WASP protein, with or without CaMKIIβ, n = 3.

(E and F) Similar experiments as those in (A) and (B) except that gelsolin was used instead of cofilin, n = 8. Kruskal-Wallis test followed by Mann-Whitney U test with Bonferroni correction was used.

All error bars represent SEM.

(Figure 2D). In actin-binding assays with gelsolin, most of the actin was found in the supernatant due to F-actin severing activity of gelsolin. However, when CaMKIIβ was present, the amount of depolymerized actin was reduced to about 37% of the level without CaMKII (84.1% ± 3.6% to 31.4% ± 1.6%; Figures 2E and 2F), suggesting an inhibitory effect of CaMKIIβ on gelsolin-mediated F-actin severing. Again, CaMKIIβ alone did not affect actin dynamics. Importantly, the All D mutant showed no effect against cofilin, Arp2/3, or gelsolin, indicating that the protective function of CaMKII is negatively regulated by phosphorylation of the F-actin binding region. Interestingly, All A shows a stronger effect on F-actin modifications than WT in assays with cofilin and gelsolin (Figures 2B, 2C, and 2F), which may result from basal phosphorylation in our CaMKIIβ WT preparation (data not shown). These results demonstrate that CaMKIIβ stabilizes F-actin by limiting access of these regulators to F-actin, which is inhibited by autophosphorylation within the F-actin binding domain.

Autophosphorylation at the F-Actin Binding Region Regulates the Accumulation and Dynamics of CaMKII in Dendritic Spines

As F-actin is the major cytoskeletal protein in the spine, we next investigated if autophosphorylation of CaMKIIβ at the F-actin binding region regulates CaMKIIβ localization and dynamics at the synapse. We first measured the spine accumulation of CaMKIIβ and its mutants, along with CaMKIIα, which does not directly interact with F-actin (Shen et al., 1998; O'Leary et al., 2006; Okamoto et al., 2007). We cotransfected GFP-CaMKII and DsRed2 into CA1 pyramidal neurons in organotypically cultured hippocampal slices (Okamoto et al., 2004) and estimated the level of spine accumulation by comparing the GFP signal in spines versus the adjoining dendritic shafts, normalized by the DsRed2 signal (Hayashi et al., 2006). GFP-CaMKIIβ WT and All A were enriched in spines compared to GFP-CaMKIIα (Figures 3A–3C). In contrast, the All D mutant showed a reduced accumulation in spines, similar to the levels of CaMKIIα (Figures 3A–3C), suggesting CaMKIIβ autophosphorylation in the F-actin binding domain controls its spine targeting. There was no change in spine density or length with any of these mutants under this condition (Figure S2).

To test whether the phosphorylation influences CaMKIIβ mobility, we analyzed the motion of individual CaMKIIβ

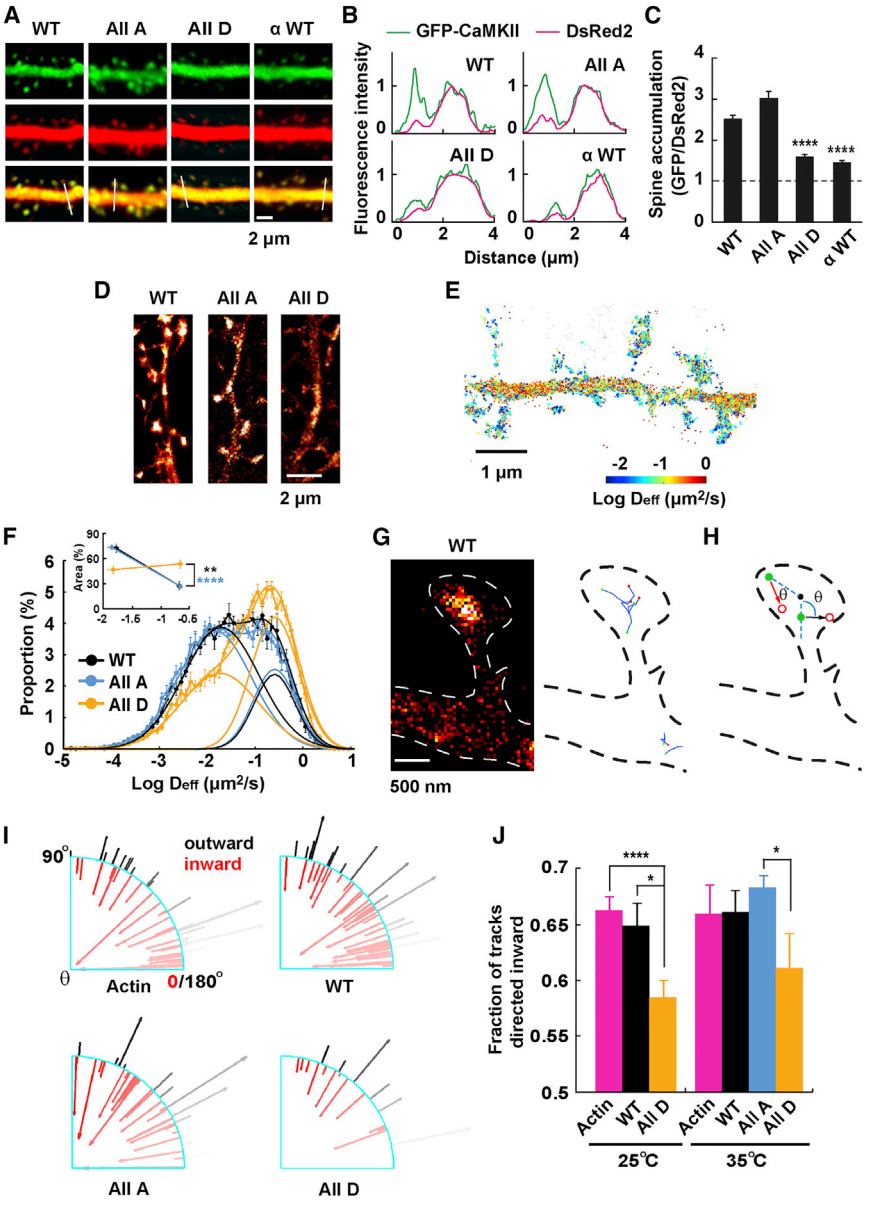

Figure 3. Autophosphorylation of the F-Actin Binding Region of CaMKIIβ Regulates F-actin Accumulation and Dynamics in Spines

(A) Distribution of GFP-CaMKIIβ WT, mutants, or CaMKIIα (green) in the apical primary dendrite of a CA1 pyramidal neuron from a hippocampal slice culture cotransfected with DsRed2 (red).

(B) The GFP and DsRed2 fluorescence intensity profiles across the line in (A). The peaks on the left of the plot correspond to the spine heads, and those on the right correspond to the dendritic shaft. The peak intensity of the dendritic shaft in the DsRed2 channel was adjusted to 1.

(C) CaMKII accumulation in spines was normalized to spine volume. The spine accumulation was determined by the fluorescence intensity of (GFP/DsRed2) spine / (GFP/DsRed2) dendrite. CaMKIIβ WT, n = 87/14 (number of spines/cells); All A, n = 60/15; All D, n = 76/15; CaMKIIα, n = 49/13.

(D) Single-molecule localization of mEos3.1-CaMKIIβ WT, All A, and All D binned at 40 nm in hippocampal dissociated culture.

(E) An example of a spatial map of molecular mobility of CaMKIIβ WT where D_{eff} was calculated and color coded.

(F) Histogram of D_{eff} of mEos3.1-CaMKIIβ WT (n = 8), All A (n = 9), and All D mutants (n = 11). The distribution was fitted with a double Gaussian curve. The individual Gaussian components are also shown. The inset shows the proportion of the area of fast and slow components. Statistical significance of WT versus All D, p = 0.00762; All A versus All D, p = 0.00068.

(G) Sample molecule trajectories of mEos3.1-CaMKIIβ (right) and a density map of all localized molecules (left). Green and red points indicate the first and last localized position, respectively.

(H) Diagram showing how track angle θ was calculated with respect to the center of the spine head to distinguish inwardly from outwardly directed molecules.

(I) Sample plots of all tracked molecules from single spines of cells transfected with the indicated constructs. The vectors show θ and velocity of each molecule. Red indicates inward tracks and black indicates outward. 0° and 180° represent directly toward and away from the center, respectively. Note that the number of the All D molecules is less than the others due to poor spine accumulation.

(J) Summary of (I), showing the fraction of tracks with inward directionality for actin (n = 31/7 spines/neurons), CaMKIIβ WT (n = 29/7), and All D (n = 35/9) at 25°C. At 35°C, actin (n = 22/7), CaMKIIβ WT (n = 47/10), All A (n = 82/18), and CaMKIIβ All D (n = 25/6). The All D mutant was statistically different from other groups (p = 0.00085, df = 3, F = 5.705). Kruskal-Wallis test followed by Mann-Whitney U test with Bonferroni correction (C and F) or two-way unbalanced Analysis of Variance followed by t test with Bonferroni correction (J) was used. See also Figure S2.

All error bars represent SEM.

molecules using single-particle tracking photoactivated localization microscopy (sptPALM) (Manley et al., 2008; Frost et al., 2010; Lu et al., 2014). The distribution of localized molecules of mEos3-CaMKIIβ WT and All A again revealed a greater enrichment within spines compared to that of the All D mutant (Figure 3D). The spatial diffusion map reveals heterogenous mobility of CaMKIIβ with lower mobility within spines than dendrites (Figure 3E). The distribution of diffusion coefficient (D_{eff}) values for mEos3-CaMKIIβ WT and All A was remarkably broad (Figure 3F). This suggests that CaMKII oligomers are subject to various factors that regulate their mobility, from nearly immobilized ($D_{eff} < 10^{-2}$ μm²/s) to diffusion with few hindrances ($D_{eff} \geq 1$ μm²/s). In contrast, the D_{eff} distribution of All D was strikingly right-shifted, predominantly exhibiting the fast diffusion typical of unbound protein (Figure 3F; inset, proportion of fast and slow components).

Actin in dendritic spines undergoes directional treadmilling (Honkura et al., 2008; Frost et al., 2010). We reasoned that

if CaMKIIβ is bound to the spine cytoskeletal network, it should show a similar directional movement determined by actin flow. We therefore analyzed the direction of motion of individual mEOS-tagged actin and CaMKIIβ molecules (Figures 3G and 3H). Consistent with previous observations, tracked actin molecules showed predominantly inward movement from the periphery of the spine toward the center (Figures 3I and 3J). Importantly, mEos3-CaMKIIβ WT showed a fraction of inwardly directed events similar to actin (0.66 ± 0.01 for actin, 0.65 ± 0.02 for CaMKIIβ WT, no statistical significance). Polar plots of molecular vectors showed a broad distribution of orientations similar to actin (Figures 3I and 3J). In contrast, All D showed reduced directional selectivity (0.58 ± 0.01; note 0.5 is expected for random movement; statistical difference was $p < 0.001$ with actin and $p < 0.05$ with CaMKIIβ WT; t test with Bonferroni correction) (Figures 3I and 3J). We also carried out experiments at physiological temperature and obtained similar results (no temperature effect with two-way unbalanced analysis of variance; df = 1, F = 0.5678, p = 0.4512). The remaining inward movement seen in All D may reflect a population interacting with F-actin indirectly through hetero-oligomerization with endogenous CaMKIIβ or proteins such as α-actinin (Hell, 2014). Overall, these results indicate that CaMKIIβ is incorporated into the dynamic F-actin network which maintains the spine structure under steady state and that autophosphorylation at the F-actin binding domain abolishes this interaction. Thus the autophosphorylation and resultant loss of CaMKII-F-actin interaction impact F-actin dynamics and spine structure.

LTP-Inducing Synaptic Stimulation Transiently Dissociates CaMKIIβ from F-Actin in Spines

Our results predict that neuronal activity and resultant autophosphorylation of CaMKIIβ cause CaMKIIβ to detach from F-actin. To visualize this process in spines, we used Förster-resonance energy transfer-fluorescence lifetime imaging microscopy (FRET-FLIM) between GFP-CaMKIIβ and mRFP-actin while stimulating the synapse with uncaging of caged glutamate which induces both functional and structural LTP in CA1 pyramidal neurons (Matsuzaki et al., 2004). To maximize the efficiency of interaction and to minimize the complications caused by overexpression, we took a molecular replacement approach, downregulating endogenous CaMKIIβ by shRNA and introducing GFP-CaMKIIβ cDNA with a silent mutation against the shRNA target (Okamoto et al., 2007).

In unstimulated spines, GFP-CaMKIIβ WT, K43R, A303R, and All A showed a significantly shorter fluorescent lifetime compared with unfused GFP, indicating that they interact with mRFP-actin in the spine (Figure 4A). Uncaging increases the lifetime of GFP-CaMKIIβ WT (i.e., decrease in the interaction between GFP-CaMKIIβ and mRFP-actin), peaking at ~20 s after the initiation of glutamate stimulation (Figures 4B and 4C). At that point, the lifetime was almost comparable to spines expressing unfused GFP, suggesting that most GFP-CaMKIIβ dissociated from mRFP-actin. The lifetime returned to basal levels after 1 min. In contrast, the All A and K43R mutants did not respond to glutamate uncaging except for a small, statistically insignificant change at the onset of stimulation. The A303R mutant did not respond to uncaging, indicating persistent interaction with F-actin. These results indicate that in vivo, autophosphorylation of the F-actin binding region plays a major role in dissociating CaMKIIβ from F-actin and the contribution of Ca^{2+}/CaM binding is small. Also, the lack of response in K43R and A303R indicates crosstalk of other kinases is unlikely. The lifetime of All D remained at a level comparable to unfused GFP throughout, consistent with the lack of interaction with F-actin (Figures 4A and S3). These results strongly support a dynamic F-actin dissociation and reassociation of CaMKIIβ upon LTP induction through an autophosphorylation-mediated mechanism.

Dissociation of CaMKIIβ from F-Actin Is Necessary for Functional and Structural LTP

To elucidate the role of CaMKIIβ detachment from F-actin during LTP, we employed the All A mutant because it displayed impaired activity-dependent dissociation from F-actin both in vitro (Figure 1G) and in vivo (Figure 4C) while maintaining normal kinase activity (Figure S1E). We first compared sLTP between neurons expressing CaMKIIβ WT and those expressing All A along with DsRed2 and CaMKIIβ shRNA. The neurons expressing CaMKIIβ WT showed sLTP similar to those expressing only DsRed2 (Cont.) (Figures 4D and 4E). In contrast, expression of All A suppressed spine enlargement. When WT and All A were coexpressed, the suppressive effects of All A occurred relative to the ratio of the two forms (Figure 4F). Similarly, the K43R and A303R also showed suppression of spine enlargement (Figure 4G), suggesting phosphorylation of the F-actin binding region of CaMKIIβ and the resulting detachment from F-actin are required for sLTP.

To confirm that the deficiency in sLTP leads to impairments in functional LTP, we electrophysiologically measured LTP in neurons expressing either WT or All A (Figure 5). We first tested if the basal synaptic transmission is changed by paired recording of transfected and adjacent untransfected neurons (Hayashi et al., 2000). The CaMKIIβ shRNA caused a significant reduction in the amplitude of AMPA-R-mediated excitatory postsynaptic current (EPSC), but not of NMDA-R-mediated EPSC, which was rescued by WT as well as All A (Figures 5A and 5B).

We then moved on to LTP induced by pairing postsynaptic depolarization and presynaptic stimulation. Expression of CaMKIIβ shRNA decreased LTP compared with untransfected neurons consistent with a study in CaMKIIβ knockout animals (Figure 5C) (Borgesius et al., 2011), which might be due to the reduction in excitatory drive (Figures 5A and 5B) and changes in postsynaptic molecular machineries (Fink et al., 2003; Okamoto et al., 2007). This reduction in LTP was rescued by expressing WT CaMKIIβ (Figures 5C and 5D). In contrast, All A failed to rescue the reduction in LTP (Figures 5C and 5D). Combined with biochemical and imaging results, we conclude that, to maintain basal transmission, the F-actin binding ability of CaMKIIβ is important, but the ability to undergo autophosphorylation in the F-actin binding region is not. The dissociation of CaMKIIβ from F-actin is specifically required for both functional and structural modification of synapses during LTP.

Specific Interruption of the CaMKIIβ-F-Actin Interaction by a Photosensitizer Protein, SuperNova

The results so far indicate that the autophosphorylation-mediated dissociation of CaMKII from F-actin is necessary for

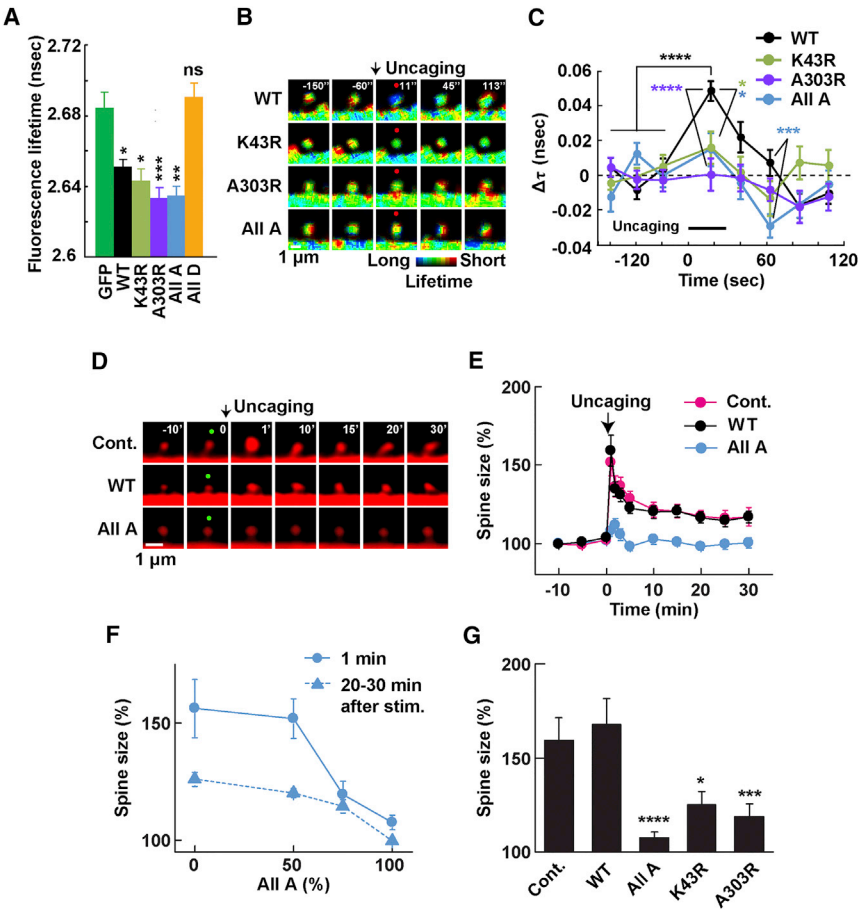

Figure 4. Inhibition of Dissociation of CaMKIIβ from F-Actin Impairs Structural LTP of Hippocampal CA1 Neurons

(A) CaMKIIβ-actin interaction monitored by FRET-FLIM. Hippocampal slice cultures were transfected with GFP or GFP-CaMKIIβ WT or mutants (all with silent mutations to make them resistant to shRNA) plus mRFP-actin along with CaMKIIβ shRNA. Fluorescence lifetime of GFP in spines was measured. CaMKIIβ WT, K43R, A303R, and All A showed basal interaction with F-actin, while All D did not. GFP, n = 122/13 (number of spines/cells); CaMKIIβ WT, n = 350/29; K43R, n = 111/11; A303R, n = 96/10; All A, n = 97/5; All D, n = 134/10.

(B and C) Induction of sLTP by glutamate uncaging causes a transient dissociation of CaMKIIβ from F-actin in a manner requiring autophosphorylation within the F-actin binding region. FLIM images of dendritic spines expressing either CaMKIIβ WT, K43R, A303R, or All A mutants before and after glutamate uncaging. Time stamp in seconds (B). Time course of lifetime change (C). CaMKIIβ WT, n = 20/6 (spines/cells); K43R, n = 19/6; A303R, n = 21/7; All A, n = 15/5.

(D–G) Inhibition of dissociation of CaMKIIβ from F-actin impairs sLTP. (D) Images of spines before and after glutamate uncaging expressing DsRed2 (Cont.), DsRed2 plus CaMKIIβ shRNA and CaMKIIβ WT, or DsRed2 plus CaMKIIβ shRNA and All A. WT and All A cDNA contained silent mutations at the shRNA target sequence. Time stamp in minutes. (E) Summary of multiple spines. Control, n = 22/12 (spines/neuron); CaMKIIβ WT, n = 21/10; All A, n = 20/10. (F) Dose dependence of All A mutant. WT and All A mutants were transfected with different ratios while keeping the total amount of plasmid DNA constant. All A 0% (WT), n = 21/10 (spines/neurons); All A 50%, n = 28/14; All A 75%, n = 16/8; All A 100%, n = 20/10. (G) Summary of spine size change, 1 min after sLTP induction. Control, n = 22/12 (spines/neurons); WT, n = 21/10; All A, n = 20/10; K43R, n = 18/4; A303R, n = 18/5. Kruskal-Wallis test followed by Mann-Whitney U test with Bonferroni correction was used in (A) and (C) between WT and mutants, and in (G). For comparison between prestimulation level and first point after stimulation in (C), Mann-Whitney U test was used. See also Figure S3.

All error bars represent SEM.

structural and functional synaptic plasticity. We finally examined if this dissociation is sufficient by itself to induce structural changes in spines. In order to specifically isolate the direct effect of CaMKIIβ dissociation in sLTP, we used a genetically encoded photosensitizer SuperNova (SN) (Takemoto et al., 2013). The excitation of a photosensitizer generates reactive oxygen species, which can inactivate proteins in close vicinity (<5 nm) of the chromophore, an effect known as chromophore-assisted light inactivation (CALI) (Linden et al., 1992). By fusing the SN directly to a protein domain that interacts with another protein of interest, we expect to specifically interrupt the protein interaction mediated by the domain it is fused to.

We replaced the kinase domain of CaMKIIβ with SN, placing SN adjacent to the F-actin binding region (SN-βΔ) to optically disrupt the interaction with F-actin by reactive oxygen species in a kinase null context (Figure 6A). We confirmed that this protein forms an oligomer similar to the full-length protein (Figure S4A). A similar fusion protein with GFP (GFP-βΔ) was enriched in spines and could rescue the change in spine structure induced by shRNA to a level comparable to full-length CaMKIIβ (Okamoto et al., 2007). We determined the two-photon excitation profile of SN and found SN has two excitation peaks, one at ~760 nm and another at >1,000 nm (Figure 6B). A hiatus was observed at 840–920 nm where imaging of other fluorescent molecules is possible without inducing CALI.

To provide evidence that SN-βΔ interacts with F-actin and detaches from it upon light activation of SN in intact cells, we expressed SN-βΔ in COS cells. The full-length GFP-CaMKIIβ WT (GFP-βWT) colocalized with F-actin labeled with Lifeact-mRuby in peripheral lamellipodia (Figure 6C). SN-βΔ and GFP-βΔ showed a similar pattern of accumulation with F-actin (Figures 6D and 6E; see Figure S4 for confirmation of binding to actin). Upon activation of GFP-βWT by bath application of Ca^{2+} ionophore ionomycin, GFP-βWT dissociated from F-actin (Figure 6C), mimicking the effect of CaMKII activation observed in purified protein and in the spine (Figures 1A, 4B, and 4C). We then tested if CALI of SN-βΔ-CFP recapitulates activation-induced dissociation from F-actin (Figures 6D, 6E, and 6H). Upon illumination, SN-βΔ-CFP detached from F-actin. F-actin also disappeared, confirming that the F-actin stabilizing effect of CaMKIIβ is lost

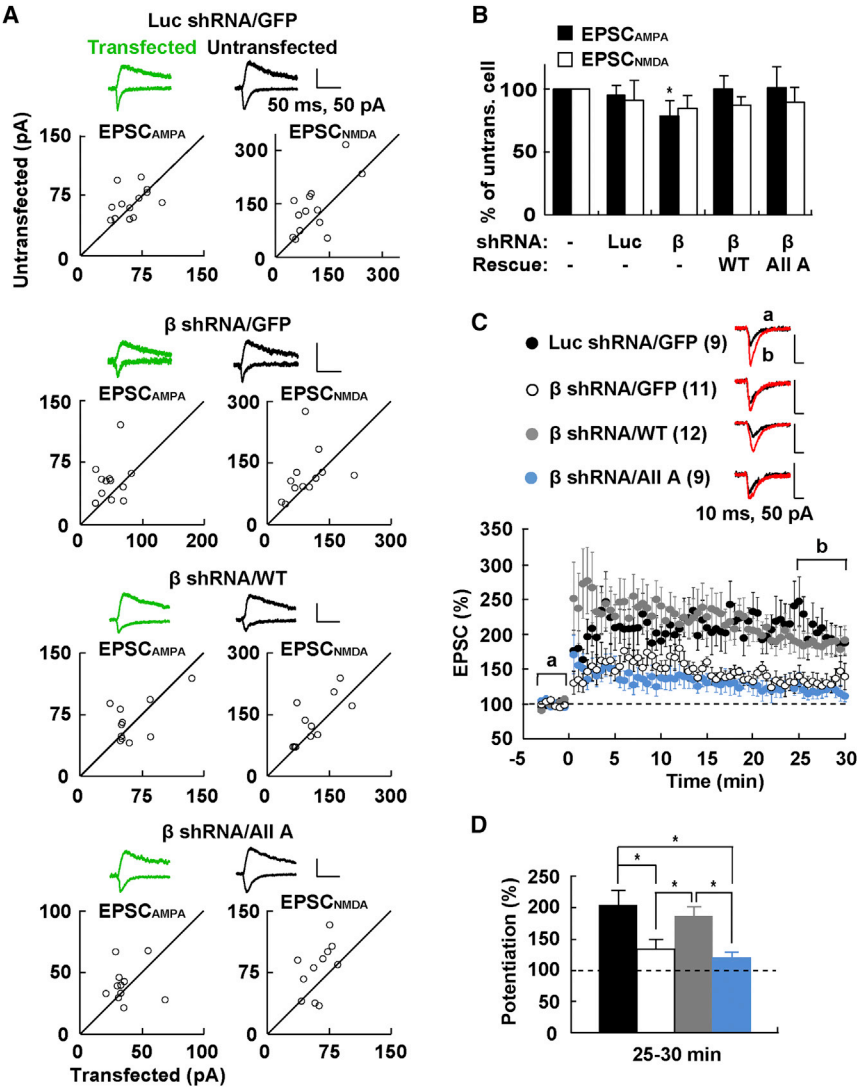

Figure 5. Impairment of sLTP by a Dissociation-Deficient CaMKIIβ Mutant Is Coupled with a Reduction in Functional LTP

(A) Pairwise analysis of the effect of transfection on AMPA- and NMDA-R-mediated synaptic transmission. Hippocampal CA1 neurons in organotypic slice culture were transfected with plasmids expressing GFP, shRNA for luciferase (control) or CaMKIIβ, and CaMKIIβ WT or All A cDNA (with silent mutations to make them resistant to shRNA). Amplitude of synaptic response from pairs of transfected and neighboring untransfected cells are plotted.

(B) Quantification of (A). There was a significant decrease in AMPA-R-mediated transmission in neurons expressing β shRNA/GFP ($p = 0.0387$, Mann-Whitney U-test). Luc shRNA/GFP, n = 13 (pairs); β shRNA/GFP, n = 12; β shRNA/WT, n = 11; β shRNA/All A, n = 11.

(C) Downregulation of CaMKIIβ with shRNA reduced LTP. CaMKIIβ WT rescued this, but All A did not. The number of cells is in parentheses. Sample traces show an average of baseline recordings (a, black) and recordings during 25–30 min (b, red).

(D) Quantification of potentiation at 25–30 min after induction of LTP (Kruskal-Wallis test followed by Mann-Whitney U test with Bonferroni correction). All error bars represent SEM.

upon CALI (Figure 6D). This is not due to photobleaching, because the average fluorescence intensity of the illuminated area was unchanged. In contrast, GFP-βΔ, which generates no reactive oxygen species, maintained colocalization with F-actin under the same illumination condition; therefore, the effect of illumination was due to the induction of CALI with SN (Figure 6E).

To test if the effect of SN is specific to the F-actin binding region, we tested a fusion of SN with full-length CaMKIIβ (SN-βWT-CFP), where SN is separated from the F-actin binding region by the kinase domain (about 6 × 4 × 3 nm) (Figure 6A). SN-βWT-CFP maintained colocalization with F-actin upon CALI under the same condition (Figures 6F and 6H), indicating a specific effect of SN on the F-actin-binding region likely due to the dependency of CALI efficacy on distance (Linden et al., 1992). Finally, the effect of CALI is not due to a direct disruptive effect of SN on F-actin, because CALI of SN-actin under the illumination condition did not change the accumulation of GFP-βWT to F-actin (Figures 6G and 6H).

Dissociation of CaMKIIβ from F-Actin Has a Permissive Role in sLTP

We next tested if we could dissociate SN-βΔ-CFP from F-actin in spines. The level of SN-βΔ-CFP was quickly reduced 1 min after CALI on a spine, but recovered after ~10 min ($\tau = 3.2$ min) (Figure 7A). This time course was consistent with the turnover time of GFP-CaMKIIβ obtained by a FRAP assay ($\tau = 3.5$ min) (Okamoto et al., 2004), reflecting the time course for exchange of molecules by diffusion. The reduced level of accumulation was comparable to the levels of SN-βΔ-CFP in the dendritic shaft (Figure 7B). In contrast, SN-βWT-CFP maintained its localization in spines, indicating the specificity of the CALI effect. These results suggest that the CALI-mediated inactivation of the F-actin binding region of CaMKIIβ can mimic the activity-induced dissociation of CaMKIIβ from F-actin in the spine.

We then tested if CALI-mediated dissociation of SN-βΔ from F-actin can change spine structure. We coexpressed SN-βΔ and GFP while downregulating endogenous CaMKIIβ with shRNA (Figures 7C and 7D). CALI in spines with SN-βΔ did not induce structural changes by itself, suggesting that acute dissociation of CaMKIIβ from F-actin is not sufficient to induce structural change of the spine. Also, uncaging alone failed to induce sLTP in spines expressing SN-βΔ (Figures 7C and 7D) or laser pulses for glutamate uncaging (without caged glutamate) did not induce CALI (Figure S5). We then combined CALI with glutamate uncaging to recruit signal transduction machinery and found that it

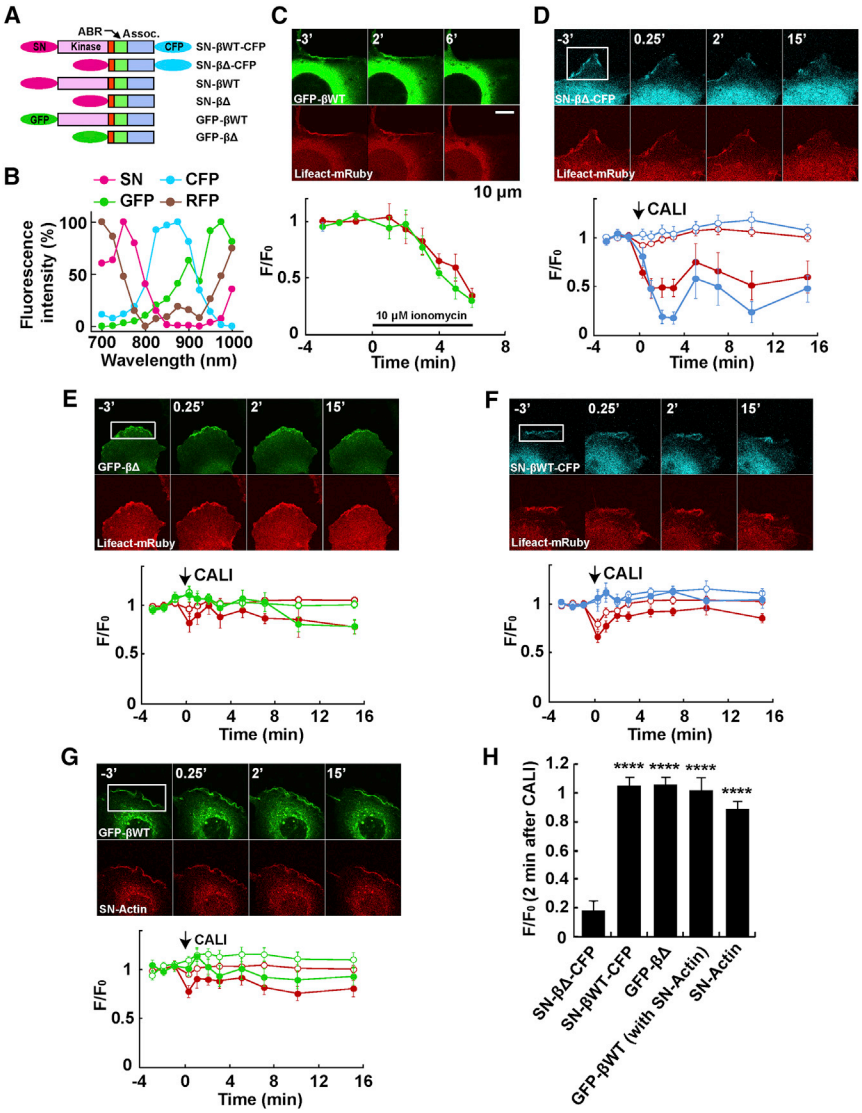

Figure 6. CALI Induced Dissociation of CaMKIIβ from F-Actin in COS Cells

(A) Domain structure of the constructs. ABR, F-actin binding region; Assoc., association domain.

(B) Two-photon excitation spectra of SuperNova (SN) and other fluorescent proteins used in CALI experiments. Emission fluorescence intensity of each protein in neuronal cell bodies was measured with two-photon excitation (10 mW, 700–1,000 nm).

(C) Dissociation of CaMKIIβ from F-actin by a Ca^{2+} ionophore. COS cells were transfected with GFP-βWT and Lifeact-mRuby. CaMKIIβ was activated by 10 μM ionomycin, and the fluorescence intensity of both CaMKIIβ (green) and Lifeact (red) at the peripheral lamellipodial region was measured (n = 9).

(D) Dissociation of SN-βΔ-CFP from F-actin by CALI. Lamellipodial region (white rectangle) was illuminated with a two-photon laser at 720 nm, 4 s. The fluorescence intensity in lamellipodium (closed circles) and the entire stimulated region (open circles) was monitored, n = 11 cells.

(E–G) Similar experiments to (D) except that cells were transfected with the indicated plasmids. In (G), visualization of SN-actin was facilitated by cotransfection of Lifeact-mRuby. GFP-βΔ, n = 9; SN-βWT-CFP, n = 8; SN-actin, n = 11.

(H) Summary of (D)–(G) at 2 min after CALI induction. Statistical significance compared with SN-βΔ-CFP by Kruskal-Wallis test followed by Mann-Whitney U test. See also Figure S4.

All error bars represent SEM.

induced a significant increase in spine volume (Figures 7C and 7D). SN-βΔ containing the All A mutation also showed similar sLTP, suggesting the phosphorylation of F-actin binding domain is not involved in the CALI-induced spine enlargement (Figure 7D). The same combination of two stimuli did not induce sLTP in spines expressing TagRFP-βΔ (deficient in CALI activity), indicating sLTP is mediated by the CALI-effect of SN. Also, this is specific to the effect on the F-actin binding region because SN fused with the full-length CaMKIIβ (with A303R mutation to block Ca^{2+}/CaM binding and kinase activation) did not induce spine volume changes. The structural effect of CALI was not mediated by a direct disruption of F-actin, because the CALI in spines expressing SN-actin did not change the spine size.

Importantly, we found that glutamate uncaging and dissociation of CaMKIIβ must occur within a time window of a few minutes. When uncaging preceded CALI, the CALI needed to be delivered within ~1 min for efficient sLTP induction (Figure 7E). This indicates that cellular signaling activated by glutamate uncaging lasts for less than a minute. When CALI preceded uncaging, uncaging needed to be delivered within 5 min (τ = 3.2 min). At 10 min after CALI, uncaging did not have an effect. This is largely consistent with the time course of recovery of SN-βΔ-CFP after CALI (Figure 7A).

We finally tested whether the dissociation of CaMKIIβ allows actin-modulating proteins to interact with F-actin within spines (Figure 7F). Cofilin-1 localization was increased in spines after CALI of SN-βΔ, but not of SN-βWT. The effect was transient, yet slightly faster than the recovery of SN-βΔ after CALI (Figure 7A), suggesting that the partial recovery of CaMKIIβ binding to the actin cytoskeleton may be sufficient for limiting access of cofilin-1. In contrast, a cofilin-1 S3D mutant, which does not interact with actin, did not show an increase in spine localization, indicating that F-actin binding localizes cofilin-1 to spines. These results suggest that CALI-mediated dissociation of CaMKIIβ from F-actin allows cofilin-1 to interact with F-actin in spines. Together, our results indicate that only when dissociation of CaMKII from F-actin is combined with cellular signaling triggered by glutamate receptor activation can modification of the spine structure occur. In other words, dissociation of CaMKIIβ from F-actin acts as a gate that permits sLTP upon Ca^{2+}-influx into dendritic spines.

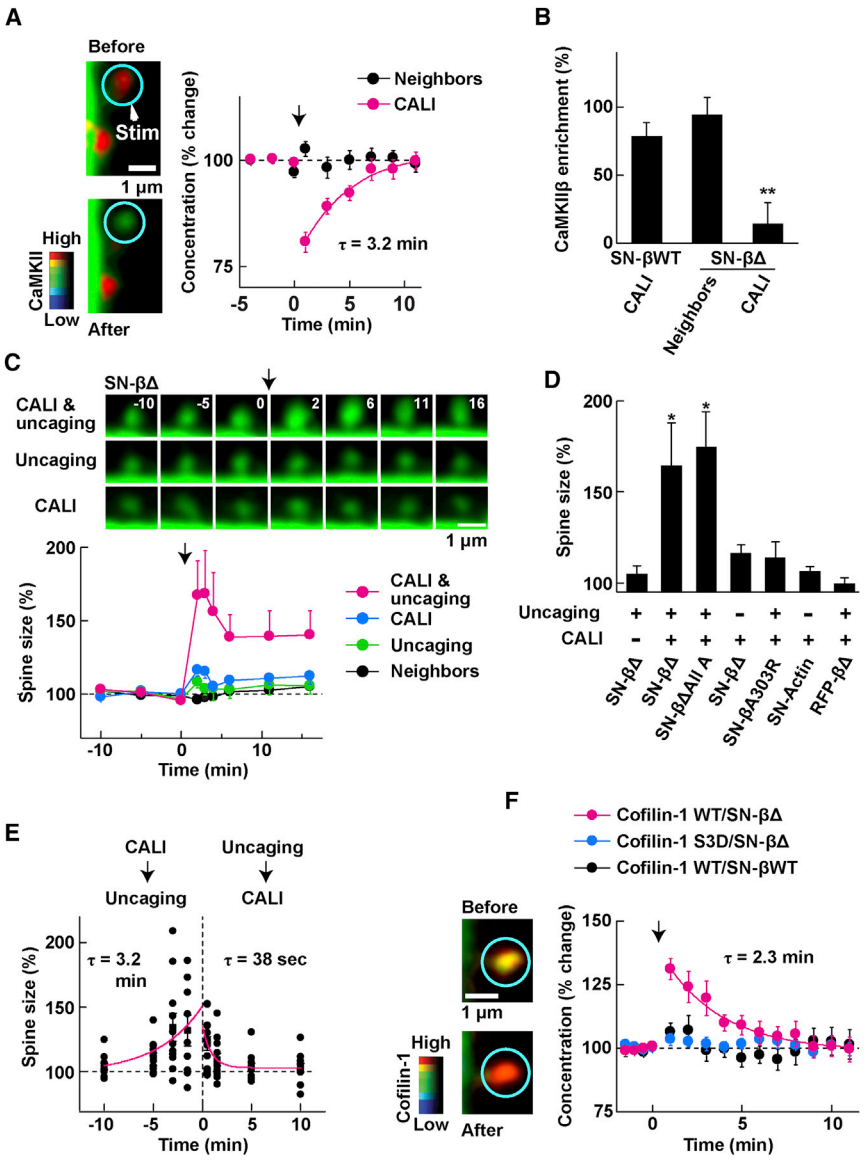

Figure 7. CaMKIIβ/F-Actin Dissociation Has a Permissive Role in the sLTP

(A) (Left) The localization of SN-βΔ-CFP before and immediately after CALI in spines. DsRed2 was coexpressed as a volume filler. Color code indicates the ratio between CFP and DsRed2 channels. A dendritic spine (circle) was illuminated with a two-photon laser at 1,000 nm, 2 s for CALI. (Right) Time course of SN-βΔ-CFP localization change in the spine after CALI. CaMKIIβ enrichment was normalized to prestimulation levels in spines. Arrow indicates the time point for CALI. The data were fitted to a single exponential curve, calculated with the first poststimulation imaging time point as zero. SN-βΔ-CFP CALI stimulated spines/neurons (CALI), n = 12/5; SN-βΔ-CFP unstimulated spines (neighbors), n = 14/5.

(B) Quantification of CALI effect on CaMKIIβ localization to dendritic spines. The average localization (%) compared to the dendrite was measured during 1–5 min after CALI. The level of SN-βΔ (or βWT)-CFP in dendritic spines and shaft before CALI was taken as 100% and 0%, respectively. CALI in SN-βΔ-CFP expressing spines/neurons, n = 12/5; neighboring spines, n = 14/5; SN-βWT-CFP, n = 13/6. Statistical significance compared with SN-βWT-CFP by Dunnett test.

(C) Effect of CALI-induced detachment of SN-βΔ on sLTP. (Top) Images of spines coexpressing SN-βΔ, GFP, and CaMKIIβ shRNA that received CALI and uncaging (top), uncaging only (middle), and CALI only (bottom). The arrow indicates the time point of glutamate uncaging and/or CALI. Timestamps in minutes. (Bottom) Time course assessment of spine size following both uncaging and CALI, n = 19/13 (spines/neurons); CALI only, n = 10/9; or uncaging only, n = 13/7. The unstimulated neighboring spines (n = 27/13) were also monitored. Spines were stimulated with glutamate uncaging immediately (<30 s) after CALI. The arrow indicates the time point of glutamate uncaging and/or CALI.

(D) Summary of data in (C). The spine size was measured 1 min after uncaging with or without CALI and normalized to prestimulation levels using GFP signal. Uncaging and CALI of SN-βΔ AII A, n = 15/9 (spines/neurons); A303R, n = 9/3; CALI only of SN-actin, n = 12/3; and uncaging and CALI of RFP-βΔ, n = 14/6. Others were the same as in (C). Statistical significance compared with SN-βΔ (uncaging only) by Dunnett test.

(E) Dependency of enlargement of dendritic spine on interval between CALI and glutamate uncaging. The spine size change was measured after 1 min of glutamate uncaging (in CALI → uncaging group) or CALI (in uncaging → CALI group). The fitting curves were obtained by a single exponential fit. Number of spines/neurons for each time point: t = −10 min, n = 11/4; −5 min, n = 10/5; −3 min, n = 11/6; −1.5 min, n = 9/4; 0.5 min, n = 15/5; 1.5 min, n = 11/4; 5 min, n = 11/5; 10 min, n = 11/4.

(F) Effect of CaMKIIβ CALI on cofilin-1 localization in spines. (Left) Subcellular localization of cofilin-1-CFP before and immediately after CaMKIIβ CALI in spines. DsRed2 was coexpressed with cofilin-1-CFP and SN-βΔ (or βWT) as a volume filler. Color coding is as in (A). (Right) Time course of change in spine cofilin-1-CFP localization. The cofilin-1 WT-CFP with SN-βΔ was fitted with single exponential. Cofilin-1 WT-CFP with SN-βΔ (cof-1 WT/SN-βΔ), n = 15/5 (spines/neurons); Cofilin-1 S3D-CFP with SN-βΔ (cof1 S3D/SN-βΔ), n = 15/6; coflin-1 WT with SN-βWT (cof-1 WT/SNβWT), n = 15/7. See also Figure S5.

All error bars represent SEM.

DISCUSSION

In this study, we identified an autophosphorylation-mediated mechanism in which CaMKII acts as a dynamic regulator of F-actin during synaptic plasticity (Figure 8). Under basal conditions, CaMKII binds F-actin and undergoes constant treadmilling to maintain spine structure. This CaMKII-F-actin interaction limits the access of actin modifying proteins and prevents their actions (Figure 8, "Basal"). Activation of CaMKII by postsynaptic Ca^{2+}-influx results in autophosphorylation of the F-actin binding region, detaching CaMKII from F-actin. This opens a time window where actin-modifying proteins

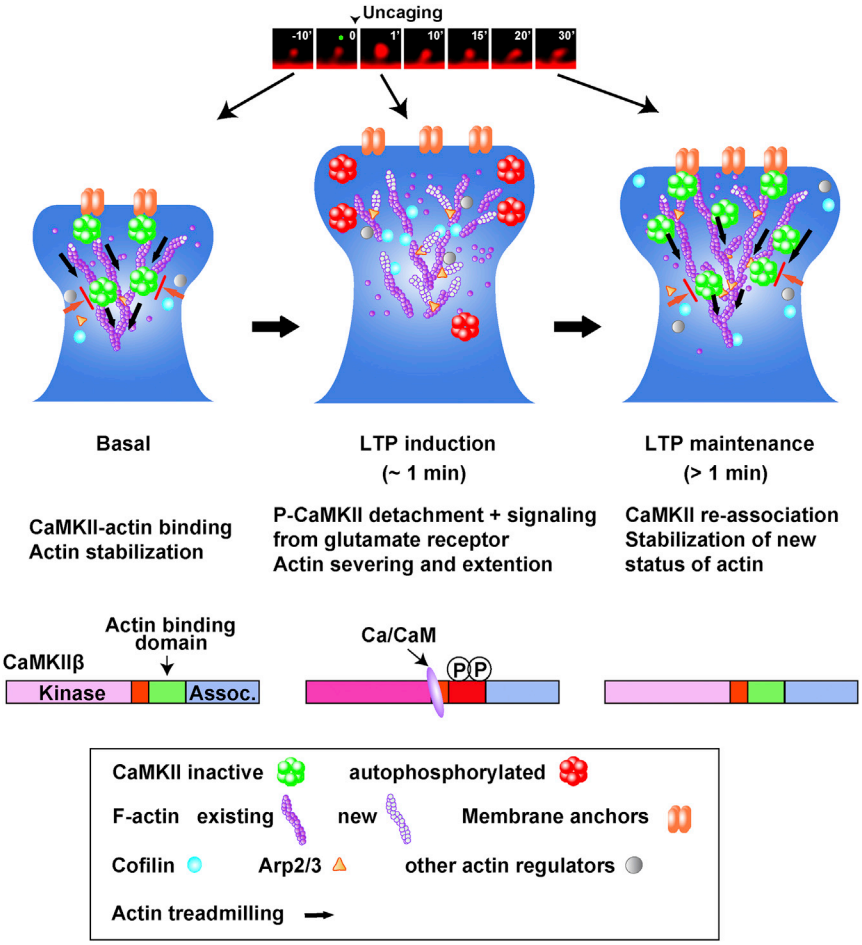

Figure 8. Role of CaMKIIβ/F-Actin as a Gate that Regulates the Structural Plasticity of Dendritic Spines

A model for the "gating" mechanism that regulates synaptic structures. Basal: at resting synapses, CaMKII bound to F-actin prevents the interaction between F-actin and actin modulating proteins (orange arrow and red line). Also, it enables structural reinforcement of F-actin by bundling and tethering it to the plasma membrane, stabilizing spine structure. LTP induction: active CaMKII autophosphorylates the F-actin binding region and dissociates from F-actin. The freed F-actin is accessible by actin modulating proteins, which are activated by a signaling cascade triggered by glutamate receptor activation. This works as a coincidence detection mechanism that results in changes in spine cytoskeletal structure. LTP maintenance: upon returning to the unphosphorylated state, CaMKII binds and bundles reorganized F-actin and maintains this remodeled spine structure.

can access and remodel F-actin (Figure 8, "LTP induction"). This time window is rather short. In our FRET-FLIM experiment, CaMKII reassociates with F-actin within a minute, thereby closing the window for structural plasticity (Figure 8, "LTP maintenance"). The dynamic, single-spine readout used in our study significantly extends previous works that indicated transient elevation of CaMKII kinase activity and the existence of kinase-independent functions (Lee et al., 2009; Okamoto et al., 2007, 2009). In CALI experiments, CaMKII-induced detachment from F-actin alone could not induce structural changes in spines, indicating it is necessary but not sufficient for sLTP (Figures 7C and 7D). Additional signaling from glutamate receptors must accompany CaMKII detachment for sLTP to occur. Considering that the time window of these two events are both short (~1 min; Figures 4 and 7), sLTP must require coincidental occurrence of both events in a spatially and temporally correlated manner. This could be a "double-verification" protective mechanism to prevent inappropriate changes in spine structure and synaptic transmission from occurring.

Subsequently, dephosphorylation by unidentified phosphatases reassociates CaMKII with F-actin, thereby restabilizing new F-actin (Figure 8, "LTP maintenance"). In this way, CaMKII serves as a gate for synaptic plasticity that permits structural modification of F-actin within spines, only when postsynaptic Ca^{2+} concentration rises sufficiently.

The F-actin binding region of CaMKIIβ has consensus sites for some other kinases. However, we do not believe such kinases are involved during LTP, because nonactivatable mutants (K43R and A303R) remained attached to F-actin upon glutamate uncaging, although their F-actin binding regions are still phosphorylatable (Figure 4C). Moreover, spines expressing these mutants showed a deficit in sLTP (Figure 4G). If other kinases mediate phosphorylation of these sites, these mutants should demonstrate similar prolonged detachment from F-actin.

Previous studies showed that different populations of actin exist in spines, from mesh-like structures localized within the spine head (Hirokawa, 1989; Korobova and Svitkina, 2010) to thick bundles, extending from the dendritic shaft into the spine neck and around the interior of the spine head (Urban et al., 2011). These different populations likely have distinct lifetimes and turnover times. A slow "enlargement pool," confined to the spine, appears upon LTP induction and is required for the long-term enlargement of spines. CaMKII inhibitor releases this pool of F-actin into the dendritic shaft, and the spine volume returns to its original size. The authors explained that CaMKII stiffens the enlargement pool of actin fibers and prevents it from passing through a narrow spine neck. It is therefore of great interest to understand how CaMKII and other actin binding proteins within spines interact with each other to generate different forms of F-actin and how they are regulated by the induction of synaptic plasticity.

In conclusion, we revealed a mechanism of cytoskeletal regulation mediated by an autophosphorylation on CaMKII, critical for gating cytoskeletal alteration within glutamatergic excitatory

synapses. This structural role of CaMKII is initiated by its kinase function and is essential to gate enlargement of spines and the enhancement of synaptic responses during LTP. Thus, the kinase-dependent and independent, structural role of CaMKII is closely linked during synaptic plasticity. The ability of CaMKIIβ to control the actin cytoskeleton in an activity-dependent fashion represents a fundamental checkpoint during synaptic plasticity. Our work sheds light on the long-standing mysteries of CaMKII-mediated molecular mechanisms that control the size and strength of synaptic connections deemed necessary for learning and memory.

EXPERIMENTAL PROCEDURES

Animal Care

Organotypic slice cultures and dissociated neuron cultures of rat hippocampus were prepared in accordance with the institutional guidelines of RIKEN BSI (Japan), the university health network animal care committee approved protocol and oversight (Canada), and the National Institutes of Health/Institutional Animal Care and Use Committee guidelines (University of Maryland School of Medicine, USA).

Fluorescence-Lifetime Measurement

GFP and mRFP were used as FRET pairs. Two-photon excitation of GFP was done with a 910 nm laser at a rate of 80 MHz, and emission light was measured via time-correlated photon counting (SPC-830, Becker and Hickl and H7422P-40, Hamamatsu Photonics), after passing through 680 nm short-pass and 510 ± 35 nm band-pass filters. The average fluorescent lifetime in the target spine head was calculated as described previously (Yasuda, 2006) using a custom written macro in Igor Pro (Wavemetrics).

CALI Using SN

For CALI experiments, we fused SN with CaMKIIβΔ (285–542) (SN-βΔ) or CaMKIIβ WT (SN-βWT) (Takemoto et al., 2013). For localization experiments, the constructs were also tagged with CFP (mTurquoise2) (SN-βΔ-CFP, SN-βWT-CFP) (Goedhart et al., 2012). In COS cells, Lifeact-mRuby was used to visualize F-actin. COS cells were transfected with SN constructs tagged with CFP and Lifeact-mRuby, and observed with a confocal microscope equipped with a 473 nm laser (for CFP excitation) and a 559 nm laser (for mRuby excitation). In a separate experiment, we confirmed that CALI does not take place with 559 nm laser for mRuby imaging. To induce CALI, we scanned the region of interest with a 720 nm two-photon laser (7 mW, 4 s).

In slice experiments, neurons were transfected with SN constructs, CaMKIIβ shRNA, and GFP or DsRed2. As a control, we used a fusion of TagRFP (Evrogen) with CaMKIIβΔ (RFP-βΔ), and also a fusion of SN with actin. The imaging was done at 900 nm. For CALI, targeted spines were exposed to a 1,000 nm two-photon laser (7 mW, 2 s) to avoid uncaging of caged glutamate. For cofilin-1 localization experiments, we fused cofilin-1 WT and S3D mutant with CFP (mTurquoise2) at the C terminus (cofilin-1-CFP).

Statistics

Statistical methods are indicated in the figure legend. Data are presented as mean ± SEM. Statistical significance is indicated in figures as *$p < 0.05$, **$p < 0.01$, ***$p < 0.005$, and ****$p < 0.001$.

SUPPLEMENTAL INFORMATION

Supplemental Information includes five figures, one table, and Supplemental Experimental Procedures and can be found with this article at http://dx.doi.org/10.1016/j.neuron.2015.07.023.

AUTHOR CONTRIBUTIONS

Y.H. and K.O. conceived experiments and contributed funding. With assistance from A.S., K.K. carried out biochemical, electrophysiological, and imaging experiments. G.L., M.K., and T.T.L. carried out imaging experiments. M.K.H. determined the phosphorylation sites. R.N. carried out a preliminary electrophysiological assay. H.E.L. and T.A.B. carried out single molecule tracking PALM. T.M. and T.N. provided SuperNova. Y.H., K.O., K.K., and T.A.B. wrote the manuscript.

ACKNOWLEDGMENTS

We thank Drs. Steve Gygi and Ross Tomaino at the Taplin Biological Mass Spectrometry Facility, Harvard Medical School, for mass spectrometric determination of phosphorylation sites; Drs. Jennifer Lippincott-Schwartz, Joachim Goedhart, Roland Wedlich-Soldner, Katsuhiko Mikoshiba, Sean McKinney, Loren Looger, and Michael Davidson for sharing materials; and Lily Yu, John Georgiou, John Lisman, Roger Colbran, Peter Scheiffele, and Yuki Goda for comments on the manuscript. This work was supported by a Grant-in-Aid for Scientific Research for Young Researchers (K.K.); by RIKEN, NIH grant R01DA17310, Grant-in-Aid for Scientific Research (A), Grant-in-Aid for Scientific Research on Innovative Area "Foundation of Synapse and Neurocircuit Pathology" from the Ministry of Education, Culture, Sports, Science and Technology of Japan, Human Frontier Science Program, and High-end Foreign Experts Recruitment Program of Guangdong Province (Y.H.); by CIHR grant MOP 111220, Canada Research Chairs Program, and Canada Foundation for Innovation (K.O.); and by NIH grant R01MH080046 (T.A.B). Y.H. is partly supported by Takeda Pharmaceutical Co. Ltd. and Fujitsu Laboratories.

Received: September 22, 2013
Revised: June 11, 2015
Accepted: July 17, 2015
Published: August 19, 2015

REFERENCES

Baucum, A.J., 2nd, Shonesy, B.C., Rose, K.L., and Colbran, R.J. (2015). Quantitative proteomics analysis of CaMKII phosphorylation and the CaMKII interactome in the mouse forebrain. ACS Chem. Neurosci. *6*, 615–631.

Borgesius, N.Z., van Woerden, G.M., Buitendijk, G.H., Keijzer, N., Jaarsma, D., Hoogenraad, C.C., and Elgersma, Y. (2011). βCaMKII plays a nonenzymatic role in hippocampal synaptic plasticity and learning by targeting αCaMKII to synapses. J. Neurosci. *31*, 10141–10148.

Bosch, M., and Hayashi, Y. (2012). Structural plasticity of dendritic spines. Curr. Opin. Neurobiol. *22*, 383–388.

Bosch, M., Castro, J., Saneyoshi, T., Matsuno, H., Sur, M., and Hayashi, Y. (2014). Structural and molecular remodeling of dendritic spine substructures during long-term potentiation. Neuron *82*, 444–459.

Brocke, L., Chiang, L.W., Wagner, P.D., and Schulman, H. (1999). Functional implications of the subunit composition of neuronal CaM kinase II. J. Biol. Chem. *274*, 22713–22722.

Calabrese, B., Saffin, J.M., and Halpain, S. (2014). Activity-dependent dendritic spine shrinkage and growth involve downregulation of cofilin via distinct mechanisms. PLoS ONE *9*, e94787.

Chen, H.X., Otmakhov, N., Strack, S., Colbran, R.J., and Lisman, J.E. (2001). Is persistent activity of calcium/calmodulin-dependent kinase required for the maintenance of LTP? J. Neurophysiol. *85*, 1368–1376.

Fink, C.C., Bayer, K.U., Myers, J.W., Ferrell, J.E., Jr., Schulman, H., and Meyer, T. (2003). Selective regulation of neurite extension and synapse formation by the β but not the α isoform of CaMKII. Neuron *39*, 283–297.

Frost, N.A., Shroff, H., Kong, H., Betzig, E., and Blanpied, T.A. (2010). Single-molecule discrimination of discrete perisynaptic and distributed sites of actin filament assembly within dendritic spines. Neuron *67*, 86–99.

Goedhart, J., von Stetten, D., Noirclerc-Savoye, M., Lelimousin, M., Joosen, L., Hink, M.A., van Weeren, L., Gadella, T.W., Jr., and Royant, A. (2012). Structure-guided evolution of cyan fluorescent proteins towards a quantum yield of 93%. Nat. Commun. *3*, 751.

Harris, K.M., Jensen, F.E., and Tsao, B. (1992). Three-dimensional structure of dendritic spines and synapses in rat hippocampus (CA1) at postnatal day 15

and adult ages: implications for the maturation of synaptic physiology and long-term potentiation. J. Neurosci. *12*, 2685–2705.

Hayashi, Y., Shi, S.H., Esteban, J.A., Piccini, A., Poncer, J.C., and Malinow, R. (2000). Driving AMPA receptors into synapses by LTP and CaMKII: requirement for GluR1 and PDZ domain interaction. Science *287*, 2262–2267.

Hayashi, M.K., Ames, H.M., and Hayashi, Y. (2006). Tetrameric hub structure of postsynaptic scaffolding protein homer. J. Neurosci. *26*, 8492–8501.

Hell, J.W. (2014). CaMKII: claiming center stage in postsynaptic function and organization. Neuron *81*, 249–265.

Hirokawa, N. (1989). The arrangement of actin filaments in the postsynaptic cytoplasm of the cerebellar cortex revealed by quick-freeze deep-etch electron microscopy. Neurosci. Res. *6*, 269–275.

Honkura, N., Matsuzaki, M., Noguchi, J., Ellis-Davies, G.C., and Kasai, H. (2008). The subspine organization of actin fibers regulates the structure and plasticity of dendritic spines. Neuron *57*, 719–729.

Hotulainen, P., and Hoogenraad, C.C. (2010). Actin in dendritic spines: connecting dynamics to function. J. Cell Biol. *189*, 619–629.

Huang, C.C., and Hsu, K.S. (2001). Progress in understanding the factors regulating reversibility of long-term potentiation. Rev. Neurosci. *12*, 51–68.

Korobova, F., and Svitkina, T. (2010). Molecular architecture of synaptic actin cytoskeleton in hippocampal neurons reveals a mechanism of dendritic spine morphogenesis. Mol. Biol. Cell *21*, 165–176.

Lee, S.J., Escobedo-Lozoya, Y., Szatmari, E.M., and Yasuda, R. (2009). Activation of CaMKII in single dendritic spines during long-term potentiation. Nature *458*, 299–304.

Lin, Y.C., and Redmond, L. (2008). CaMKIIβ binding to stable F-actin in vivo regulates F-actin filament stability. Proc. Natl. Acad. Sci. USA *105*, 15791–15796.

Linden, K.G., Liao, J.C., and Jay, D.G. (1992). Spatial specificity of chromophore assisted laser inactivation of protein function. Biophys. J. *61*, 956–962.

Lisman, J., Yasuda, R., and Raghavachari, S. (2012). Mechanisms of CaMKII action in long-term potentiation. Nat. Rev. Neurosci. *13*, 169–182.

Lu, W., Man, H., Ju, W., Trimble, W.S., MacDonald, J.F., and Wang, Y.T. (2001). Activation of synaptic NMDA receptors induces membrane insertion of new AMPA receptors and LTP in cultured hippocampal neurons. Neuron *29*, 243–254.

Lu, H.E., MacGillavry, H.D., Frost, N.A., and Blanpied, T.A. (2014). Multiple spatial and kinetic subpopulations of CaMKII in spines and dendrites as resolved by single-molecule tracking PALM. J. Neurosci. *34*, 7600–7610.

Malenka, R.C., Lancaster, B., and Zucker, R.S. (1992). Temporal limits on the rise in postsynaptic calcium required for the induction of long-term potentiation. Neuron *9*, 121–128.

Manley, S., Gillette, J.M., Patterson, G.H., Shroff, H., Hess, H.F., Betzig, E., and Lippincott-Schwartz, J. (2008). High-density mapping of single-molecule trajectories with photoactivated localization microscopy. Nat. Methods *5*, 155–157.

Matsuzaki, M., Ellis-Davies, G.C., Nemoto, T., Miyashita, Y., Iino, M., and Kasai, H. (2001). Dendritic spine geometry is critical for AMPA receptor expression in hippocampal CA1 pyramidal neurons. Nat. Neurosci. *4*, 1086–1092.

Matsuzaki, M., Honkura, N., Ellis-Davies, G.C., and Kasai, H. (2004). Structural basis of long-term potentiation in single dendritic spines. Nature *429*, 761–766.

Miller, S.G., Patton, B.L., and Kennedy, M.B. (1988). Sequences of autophosphorylation sites in neuronal type II CaM kinase that control Ca^{2+}-independent activity. Neuron *1*, 593–604.

O'Leary, H., Lasda, E., and Bayer, K.U. (2006). CaMKIIβ association with the actin cytoskeleton is regulated by alternative splicing. Mol. Biol. Cell *17*, 4656–4665.

Okamoto, K., Nagai, T., Miyawaki, A., and Hayashi, Y. (2004). Rapid and persistent modulation of actin dynamics regulates postsynaptic reorganization underlying bidirectional plasticity. Nat. Neurosci. *7*, 1104–1112.

Okamoto, K., Narayanan, R., Lee, S.H., Murata, K., and Hayashi, Y. (2007). The role of CaMKII as an F-actin-bundling protein crucial for maintenance of dendritic spine structure. Proc. Natl. Acad. Sci. USA *104*, 6418–6423.

Okamoto, K., Bosch, M., and Hayashi, Y. (2009). The roles of CaMKII and F-actin in the structural plasticity of dendritic spines: a potential molecular identity of a synaptic tag? Physiology (Bethesda) *24*, 357–366.

Pontrello, C.G., and Ethell, I.M. (2009). Accelerators, brakes, and gears of actin dynamics in dendritic spines. Open Neurosci. J. *3*, 67–86.

Saito, A., Miyajima, K., Akatsuka, J., Kondo, H., Mashiko, T., Kiuchi, T., Ohashi, K., and Mizuno, K. (2013). CaMKIIβ-mediated LIM-kinase activation plays a crucial role in BDNF-induced neuritogenesis. Genes Cells *18*, 533–543.

Sanabria, H., Swulius, M.T., Kolodziej, S.J., Liu, J., and Waxham, M.N. (2009). βCaMKII regulates actin assembly and structure. J. Biol. Chem. *284*, 9770–9780.

Saneyoshi, T., and Hayashi, Y. (2012). The Ca^{2+} and Rho GTPase signaling pathways underlying activity-dependent actin remodeling at dendritic spines. Cytoskeleton *69*, 545–554.

Schikorski, T., and Stevens, C.F. (1997). Quantitative ultrastructural analysis of hippocampal excitatory synapses. J. Neurosci. *17*, 5858–5867.

Shen, K., and Meyer, T. (1999). Dynamic control of CaMKII translocation and localization in hippocampal neurons by NMDA receptor stimulation. Science *284*, 162–166.

Shen, K., Teruel, M.N., Subramanian, K., and Meyer, T. (1998). CaMKIIβ functions as an F-actin targeting module that localizes CaMKIIα/β heterooligomers to dendritic spines. Neuron *21*, 593–606.

Takemoto, K., Matsuda, T., Sakai, N., Fu, D., Noda, M., Uchiyama, S., Kotera, I., Arai, Y., Horiuchi, M., Fukui, K., et al. (2013). SuperNova, a monomeric photosensitizing fluorescent protein for chromophore-assisted light inactivation. Sci. Rep. *3*, 2629.

Trinidad, J.C., Thalhammer, A., Specht, C.G., Schoepfer, R., and Burlingame, A.L. (2005). Phosphorylation state of postsynaptic density proteins. J. Neurochem. *92*, 1306–1316.

Urban, N.T., Willig, K.I., Hell, S.W., and Nägerl, U.V. (2011). STED nanoscopy of actin dynamics in synapses deep inside living brain slices. Biophys. J. *101*, 1277–1284.

Yasuda, R. (2006). Imaging spatiotemporal dynamics of neuronal signaling using fluorescence resonance energy transfer and fluorescence lifetime imaging microscopy. Curr. Opin. Neurobiol. *16*, 551–561.